Communications in Advanced Mathematical Sciences
Vol. 5, No. 2, 92-98, 2022
Research Article
e-ISSN: 2651-4001
DOI: 10.33434/cams.1064713

On Bifurcations Along the Spiral Organization of the Periodicity in a Hopfield Neural Network

Angela da Silva, Paulo C. Rech*

Abstract
In this paper we report numerical results with respect to a certain Hopfield-type three-neurons network, where the activation function is of the type hyperbolic tangent function. Specifically, we investigate a place in a two-dimensional parameter-space of this system where typical periodic structures, the so-called shrimps, are embedded in a chaotic region. We show that these periodic structures are self-organized as a spiral that coil up toward a focal point, while undergo period-adding bifurcations. We also indicate the locations along this spiral in the parameter-space, where such bifurcations happen.

Keywords: Chaos, Lyapunov Exponents Spectrum, Parameter-Space, Period-Adding Bifurcation.
2010 AMS: 65-XX, 65Pxx, 65P20

Departamento de Física, Universidade do Estado de Santa Catarina, 89219-710 Joinville, Brazil
***Corresponding author**: paulo.rech@udesc.br
Received: 31 January 2022, **Accepted:** 27 June 2022, **Available online:** 30 June 2022

1. Introduction

A Hopfield neural network [1] is an important mathematical model in artificial neurocomputing [2]. It is a continuous-time nonlinear dynamical system which is modeled by a set of n autonomous first-order nonlinear ordinary differential equations given by

$$C_i\dot{x}_i = -\frac{x_i}{R_i} + \sum_{j=1}^{n} w_{ij}v_j + I_i, \quad i = 1,2,\ldots,n, \tag{1.1}$$

where $v_j = f_j(x_j)$, x_i are real dynamical variables, C_i, R_i, and I_i are control parameters, and w_{ij} are the elements of an $n \times n$ matrix, namely the weight matrix or the connectivity matrix, which describes the strength of the connections between the n neurons that make up the network. The neuron activation function $f_j(x_j)$ is a bounded monotonic differentiable function usually represented by any smooth function.

A low-dimensional form of the mathematical model (1.1) is investigated here, namely the one concerned with a system composed of three neurons, and whose behavior depends on two control parameters, α and γ, and which is given by

$$\begin{aligned}
\dot{x}_1 &= -x_1 + 1.5f_1(x_1) + 2.9f_2(x_2) + \alpha f_3(x_3),\\
\dot{x}_2 &= -x_2 - 1.5f_1(x_1) + 1.18f_2(x_2),\\
\dot{x}_3 &= -x_3 + \gamma f_1(x_1) - 22f_2(x_2) + 0.47f_3(x_3).
\end{aligned} \tag{1.2}$$

To obtain system (1.2), we consider in system (1.1) the weight matrix equal to

$$\begin{pmatrix} 1.5 & 2.9 & \alpha \\ -1.5 & 1.18 & 0 \\ \gamma & -22 & 0.47 \end{pmatrix},$$

$n = 3$, $C_i = R_i = 1$ and $I_i = 0$, for $i = 1,2,3$. The neuron activation function considered in our study, which defines the nonlinearity in system (1.2), is a single hyperbolic tangent function given by $f_j(x_j) = \tanh(x_j)$, plotted in Fig. 1.1 in order to illustrate.

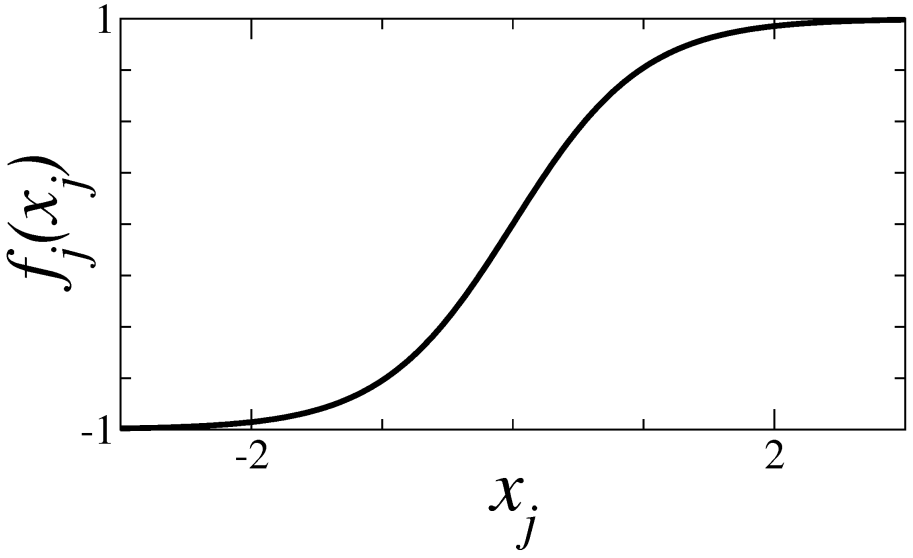

Figure 1.1. The hyperbolic tangent activation function that stands for the nonlinearity in system (1.2).

Huang and Huang [3] present various results concerning system (1.2), with the parameter α kept fixed at 0.8, involving mainly Lyapunov exponents, bifurcation diagrams, and attractors in the phase-space. Periodic and chaotic attractors were reported in [3], as a function of an other parameter (β), namely that which is the coefficient of the term $f_1(x_1)$ in the $\dot{x}_2$ equation in system (1.2). Therefore, the investigation carried out concerning system (1.2) and reported in [3] considered only a small quantity of points in a two-dimensional (α,β) parameter-space, more specifically those points located along the straight line α=0.8. A system similar to system (1.2), with a different weight matrix was presented by Chen and co-workers [4]. This time the dynamics of the system was investigated again varying only one parameter, by means of Lyapunov exponents spectra, phase-space portraits, and bifurcation diagrams. The authors present a numerical verification of the existence of a horseshoe in this system, for a certain parameter value. Lyapunov exponents spectrum, power spectrum, bifurcation diagrams, and topological horseshoe theory were used by Zheng and co-workers [5] to numerically investigate another three-neuron one-parameter chaotic Hopfield-type network with the hyperbolic tangent as the activation function. The existence of a horseshoe in the system was proved for a certain value of the variable parameter.

A two-dimensional parameter-space of system (1.2) was investigated by Mathias and Rech [6, 7]. However, the parameters and/or ranges of parameters considered there are different from those we consider here. Reference [6] also considers a piecewise-linear function as the activation function, by replacing the hyperbolic tangent function. The parameter-spaces obtained by using the two activation functions, obviously one at a time, are compared in Mathias and Rech [6], being the existence of organized periodic structures embedded in chaotic regions verified in both cases.

The main objective in this work is to investigate a particular region of the two-dimensional (α,γ) parameter-space of system (1.2), where we have detected a spiral periodic structure that coil up toward a focal point, while undergo period-adding bifurcations. More specifically, we are interested in making a numerical estimate of the location of the points along this spiral, where the involved bifurcations occur. The paper is organized as follows. In Sect. 2 we present and discuss a parameter-space diagram related with the model (1.2), which show different colored regions signifying different dynamical behaviors, namely chaotic and periodic. Finally, concluding remarks are given in Sect. 3.

2. Numerical Results

Figure 2.1(a) shows a global view of the (α, γ) parameter-space of system (1.2), namely for $0.4 \leq \alpha \leq 1.2$ and $-5 \leq \gamma \leq 15$,

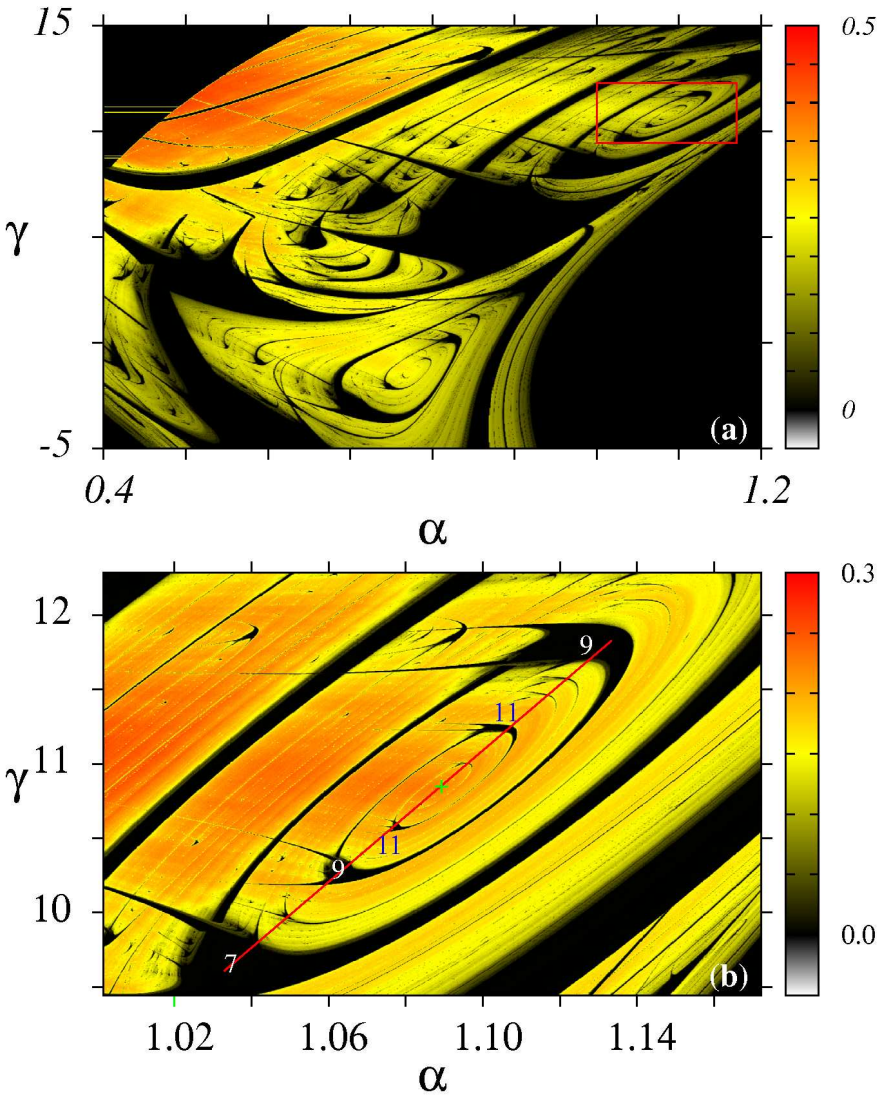

Figure 2.1. (a) Global view of the (α,γ) parameter-space of system (1.2), showing different dynamical behaviors. (b) Amplification of the boxed region in (a). Numbers refer to periods (see the text).

while in Fig. 2.1(b) one can see a particular region, that within the boxed region in Fig. 2.1(a) for which $1.00 \leq \alpha \leq 1.17$ and $9.44 \leq \gamma \leq 12.28$. Color in diagrams of Fig. 2.1 is related to the magnitude of the respective largest Lyapunov exponent (LLE). A positive LLE is indicated by a continuously changing yellow to red color, a negative LLE is indicated by a continuously changing white to black color, and the black color itself indicates a zero LLE, according to the scale shown in the column at right side in the diagram. Therefore, each point in Fig. 2.1 was painted according to the dynamical behavior presented, which was characterized by the related LLE. A chaotic region, for which the LLE is greater than zero, is painted in yellow-red, while a periodic region, for which the LLE is equal to zero, is painted in black.

Diagrams in Fig. 2.1 were obtained by computing the LLE on a grid of $10^3 \times 10^3$ (α,γ) parameters, always using an algorithm based in that present in Wolf and co-workers [8]. For each of the one million parameter sets (one million points in each diagram of Fig. 2.1), system (1.2) was integrated by using a fourth order Runge-Kutta algorithm, with a fixed time step size equal to 10^{-2}, being dropped the first 1×10^6 integration steps, regarded as a transient. For the computation of the average involved in the calculation of each one of the one million LLE, were considered the subsequent 1×10^6 integration steps.

Integrations were performed along lines of a constant parameter γ, starting always at the minor value of the parameter α. For instance, the diagram in Fig. 2.1(b) was constructed from an arbitrary initial condition for a fixed pair of parameters, in fact the two lowest $\alpha = 1.00$ and $\gamma = 9.44$. The variables (x_1, x_2, x_3) at the end of the integration for this pair of parameters were used to initialize the integration for the next pair, and so forth up to the highest value of both parameters, namely $\alpha = 1.17$ and $\gamma = 12.28$, be achieved. In other words, the procedure *following the attractor* along lines of fixed γ was used.

Both diagrams in Fig. 2.1 show dynamical behaviors of the Hopfield neural network (1.2), where we identify an intricate mixture of chaotic and periodic regions, represented respectively by yellow-red and black colors. They indicate how variations in the connection weight α, between third and first neurons, and γ, between first and third neurons, affect the dynamical behavior of the system (1.2). Figures 2.1(a) and 2.1(b) may be interpreted, each one of them, as presenting a chaotic region, in yellow-red, with several periodic regions in black, embedded in it. In other words, as the parameters α and γ are varied, we may observe regions on the (α,γ) parameter-space, where periodic structures appear embedded in a chaotic region.

Numbers identifying some periodic structures in black in Fig. 2.1(b) refer to the lower period (henceforth referred as period) of the respective structure, once bifurcations may occur when we move from the center to the periphery of each periodic structure. Period here is assumed as being the number of local maxima of the variable x_3, represented by X_3, in one complete trajectory on the phase-space attractor.

Some features, concerned with the above-mentioned periodic structures embedded in the chaotic region of the (α,γ) parameter-space in Figs. 2.1(a) and 2.1(b), deserve prominence and will be discussed in the continuation. For instance, it is remarkable the arrangement of periodic structures in the form of a spiral, that appears embedded in the chaotic set inside the boxed region in Fig. 2.1(a), and that appears amplified in Fig. 2.1(b). Note in Fig. 2.1(b) that this spiral structure coil up clockwise around a focal point marked with the plus sign in green, where the spiral itself initiates or terminates. By walking clockwise along this spiral in Fig. 2.1(b), moving along the *leg* joined to the period-7 structure at the lower portion of the parameter-space, we arrive at the period-9 structure at the upper portion. Continuing the moving, now from this period-9 structure, along the *leg* joined to it, we arrive at the period-9 structure at the lower portion. As can be concluded from inspection of Fig. 2.1(b), this behavior is recurrent, and the result is the $\ldots 7 \to 9 \to 9 \to 11 \to 11 \to 13 \to 13 \to \ldots$ periodic sequence, as we move along the *legs* of the periodic structures, closer and closer to focal point of the spiral. Therefore, this result may be interpreted as a period-adding sequence, whose increment in the period is equal to two, as the spiral is covered towards its focal point.

Numbers identifying the periods of some structures in Fig. 2.1(b) were determined with the assistance of the bifurcation diagram in Fig. 2.2, which was constructed by considering points along the red straight line $\gamma = 22.11\alpha - 12.50$ in Fig. 2.1(b),

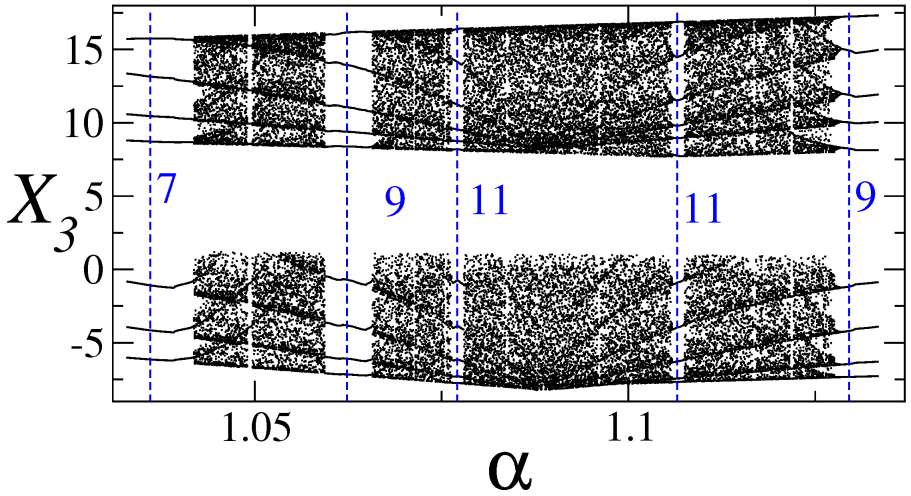

Figure 2.2. Bifurcation diagram for points along the red straight line $\gamma = 22.11\alpha - 12.50$ in Fig. 2.1(b), with $1.03293 \leq \alpha \leq 1.13337$. For each value of α was plotted the number of local maxima of the variable x_3, namely X_3, in one complete trajectory on the phase-space attractor.

for $1.03293 \leq \alpha \leq 1.13337$. Diagram in Fig. 2.2 considers the number of local maxima of the variable x_3 in one complete trajectory on the phase-space attractor, as a function of the parameter α. For each of the 10^3 values of the parameter α, were plotted 60 values of the local maximum X_3. As can be easily checked, each periodic window in Fig. 2.2 is related to a periodic structure of same number and position in Fig. 2.1(b).

Such spiral organization was observed before in different systems, modeled by different sets of nonlinear first-order ordinary differential equations, involving different mathematical functions. Some examples include electronic circuits [9, 10, 11], the Rössler model [12], a chemical oscillator [10], modified optical injection semiconductor lasers [13], a tumor growth model [14], an ecological model [15], the Lorenz-Stenflo system [16], and a thermal convection system [17], just to mention a few. The global mechanism behind the origin of the spiral organization of periodic structures in two dimensional parameter-spaces was reported simultaneously by Barrio and co-workers [18] and Vitolo and co-workers [19], having already been carried out experimental observation of such structures in electronic circuits [20].

Figure 2.3(a) shows the same particular region of the (α,γ) parameter-space of system (1.2) shown in Fig. 2.1(b), namely

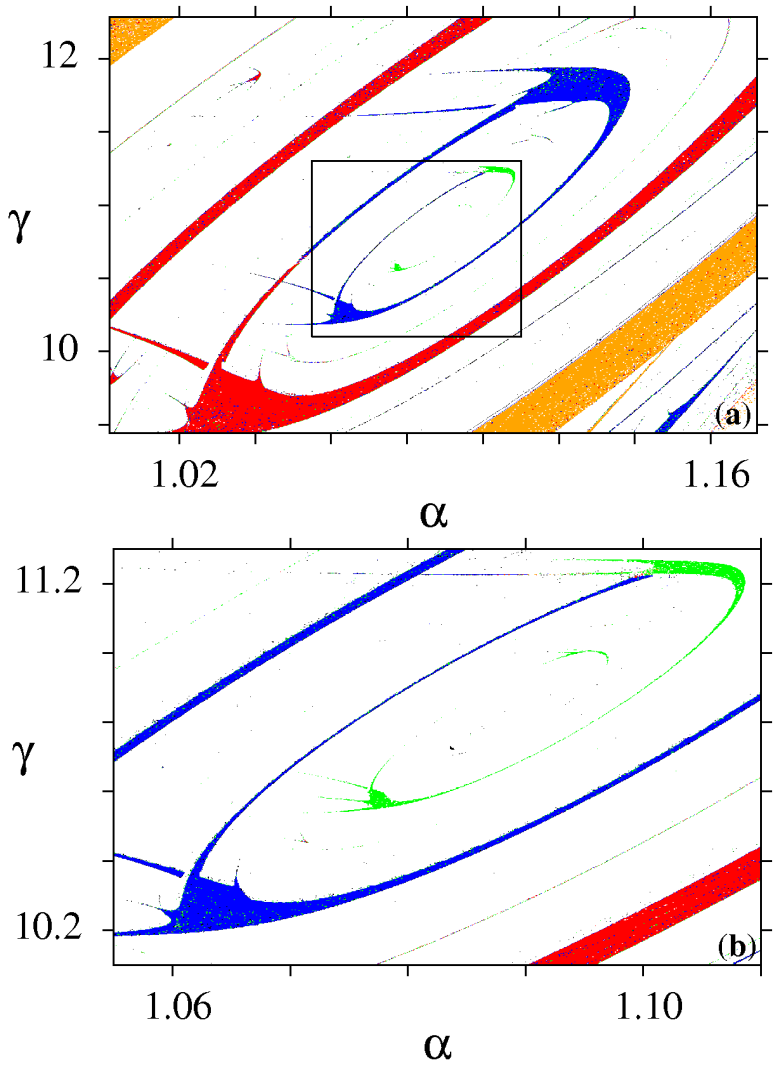

Figure 2.3. Both diagrams show periodic and chaotic behaviors in the (α,γ) parameter-space of system (1.2), with a hyperbolic tangent as the neuron activation function. Orange, red, blue, and green are associated respectively to periods 5, 7, 9, and 11.

for $1.00 \leq \alpha \leq 1.17$ and $9.44 \leq \gamma \leq 12.28$, while in Fig. 2.3(b) is shown an enlargement of the region inside the box in Fig. 2.3(a), for $1.055 \leq \alpha \leq 1.11$ and $10.1 \leq \gamma \leq 11.3$. Both plots are periodicity diagrams in the (α,γ) parameter-space, *i.e.*, the dynamical characterization of each point was made by using the period of the related trajectory in the phase-space, instead of the LLE. Therefore, each diagram in Fig. 2.3 provide us with more information than the one in Fig. 2.1(b), since the former discriminate different periodic regions and chaos, while the second only discriminate chaotic and periodic regions. As we said before, period is defined as the number of local maxima of the variable x_3 in one complete trajectory on the phase-space attractor. A period-k orbit is detected when $|(X_3)_k - (X_3)_0| < |(X_3)_0/10^3|$, $k = 1,2,\ldots$.

Color in diagrams of Fig. 2.3 is related to the period of the respective structure. Period-5, period-7, period-9, and period-11 structures are painted respectively in orange, red, blue, and green. Structures with other period values are painted in white, as well as the chaotic regions. As before in obtaining diagrams in Fig. 2.1, system (1.2) was integrated by using a fourth order Runge-Kutta algorithm, with a fixed time step size equal to 10^{-2}, being dropped the first 1×10^6 integration steps, regarded as a transient. After this integration time, subsequent few integration steps were considered to determine the period for each pair of parameters (α,γ) in diagrams of Fig. 2.3.

In addition to discriminating different periods and chaos, diagrams in Fig. 2.3 provide us with additional information regarding the bifurcations that occur as the spiral is traversed in the direction of its focal point. As can be seen in Fig. 2.3(a), the bifurcation $7 \to 9$ occurs along the *leg* joining the period-7 and period-9 structures, where the color changes from red to blue. Figure 2.3(b) shows that the bifurcation $9 \to 11$ occurs along the *leg* joining the period-9 and period-11 structures,

where the color changes from blue to green. Enlargement in an suitable region of Fig. 2.3(b) would show the location of the bifurcation $11 \to 13$, along the *leg* joining the period-11 and period-13 structures. Continuing with this procedure, *i.e.*, by producing enlargement in a suitable region of the previously obtained figure, which is not shown here, it would be possible to see the location of the bifurcation $13 \to 15$. Therefore, it is not difficult to conclude that the locations of the bifurcations $13 \to 15$, $15 \to 17$, $17 \to 19$, and so on, can be determined by considering different length scales in the (α, γ) parameter-space of system (1.2), *i.e.*, by considering diagrams resulting from enlargements of enlargements in Fig. 2.3(b).

3. Summary

In this work we have investigated a Hopfield-type three-neurons network, with a hyperbolic tangent function as the activation function. We have found a place in a two-dimensional parameter-space of this system, where typical periodic structures, the so-called shrimps, are embedded in a chaotic region, organized themselves in a spiral that coil up toward a focal point, while period-adding bifurcations occur. We have indicated the location along this spiral in the parameter-space, where these bifurcations happen.

Acknowledgements

The authors would like to express their sincere thanks to the editor and the anonymous reviewers for their helpful comments and suggestions.

Funding

Conselho Nacional de Desenvolvimento Científico e Tecnológico-CNPq, and Fundação de Amparo à Pesquisa e Inovação do Estado de Santa Catarina-FAPESC, Brazilian Agencies.

Availability of data and materials

Not applicable.

Competing interests

The authors declare that they have no competing interests.

Author's contributions

All authors contributed equally to the writing of this paper. All authors read and approved the final manuscript.

References

[1] J. J. Hopfield, *Neurons with graded response have collective computational properties like those of two-state neurons*, Proc. Natl. Acad. Sci. USA, **81** (1984), 3088–3092.

[2] E. Korner, R. Kupper, M. K. M. Rahman, Y. Shkuro, *Neurocomputing Research Developments*, Nova Science Publishers, New York, 2007.

[3] W. Z. Huang, Y. Huang, *Chaos, bifurcations and robustness of a class of Hopfield neural networks*, Int. J. Bifurcation and Chaos, **21** (2011), 885–895.

[4] P. F. Chen, Z. Q. Chen, and W. J. Wu, *A novel chaotic system with one source and two saddle-foci in Hopfield neural networks*, Chin. Phys. B, **19** (2010), 040509.

[5] P. Zheng, W. Tang, J. Hang, *Some novel double-scroll chaotic attractors in Hopfield networks*, Neurocomputing, **73** (2010), 2280–2285.

[6] A. C. Mathias and P. C. Rech, *Hopfield neural network: The hyperbolic tangent and the piecewise-linear activation functions*, Neural Networks, **34** (2012), 42–45.

[7] P. C. Rech, *Period-adding and spiral organization of the periodicity in a Hopfield neural network*, Int. J. Mach. Learn. & Cyber., **6** (2015), 1–6.

[8] A. Wolf , J. B. Swift, H. L. Swinney, and J. A. Vastano, *Determining Lyapunov exponents from a time series*, Physica D, **16** (1985), 285–317.

[9] C. Bonatto, J. A. C. Gallas, *Periodicity hub and nested spirals in the phase diagram of a simple resistive circuit*, Phys. Rev. Lett., **101** (2008), 054101.

[10] J. A. C. Gallas, *The structure of infinite periodic and chaotic hub cascades in phase diagrams of simple autonomous flows*, Int. J. Bifurcation and Chaos, **20** (2010), 197–211.

[11] H. A. Albuquerque, P. C. Rech, *Spiral periodic structure inside chaotic region in parameter-space of a Chua circuit*, Int. J. Circ. Theor. Appl., **40** (2012), 189–194.

[12] R. Barrio, F. Blesa, S. Serrano, *Qualitative analysis of the Rössler equations: Bifurcations of limit cycles and chaotic attractors*, Physica D, **238** (2009), 1087–1100.

[13] X. F. Li, Y. T. L. Andrew, Y. D. Chu, *Symmetry and period-adding windows in a modified optical injection semiconductor laser model*, Chin. Phys. Lett., **29** (2012), 010201.

[14] C. Stegemann, P. C. Rech, *Organization of the dynamics in a parameter plane of a tumor growth mathematical model*, Int. J. Bifurcation and Chaos, **24** (2014), 1450023.

[15] R. A. da Silva, P. C. Rech, *Spiral periodic structures in a parameter plane of an ecological model*, Appl. Math. Comput., **254** (2015), 9–13.

[16] P. C. Rech, *Spiral organization of periodic structures in the Lorenz-Stenflo system*, Phys. Scr., **91** (2016), 075201.

[17] A. da Silva, P. C. Rech, *Numerical investigation concerning the dynamics in parameter planes of the Ehrhard-Müller System*, Chaos Solitons Fractals, **110** (2018), 152–157.

[18] R. Barrio, F. Blesa, S. Serrano, A. Shilnikov, *Global organization of spiral structures in biparameter space of dissipative systems with Shilnikov saddle-foci*, Phys. Rev. E, **84** (2011), 035201.

[19] R. Vitolo, P. Glendinning, J. A. C. Gallas, *Global structure of periodicity hubs in Lyapunov phase diagrams of dissipative flows*, Phys. Rev. E, **84** (2011), 016216.

[20] R. Stoop, P. Benner, Y. Uwate, *Real-world existence and origins of the spiral organization of shrimp-shaped domains*, Phys. Rev. Lett., **105** (2010), 074102.